RESEARCH ARTICLE | FEBRUARY 27 2020

Polymer foil windows for gas–vacuum separation in accelerator applications

J. Engel ; M. Gross ; G. Koss; O. Lishilin ; G. Loisch ; S. Philipp; D. Richter; F. Stephan

AIP Advances 10, 025224 (2020)
https://doi.org/10.1063/1.5143258

Polymer foil windows for gas–vacuum separation in accelerator applications

Cite as: AIP Advances 10, 025224 (2020); doi: 10.1063/1.5143258
Submitted: 20 December 2019 • Accepted: 3 February 2020 •
Published Online: 27 February 2020

J. Engel,[1,a] M. Gross, G. Koss, O. Lishilin,[1] G. Loisch,[1,b] S. Philipp,[1] D. Richter,[2] and F. Stephan[1]

AFFILIATIONS

[1] Deutsches Elektronen Synchrotron DESY, Platanenallee 6, 15738 Zeuthen, Germany
[2] Helmholtzzentrum Berlin, Albert-Einstein-Str. 15, 12489 Berlin, Germany

[a] **Present address:** University Leipzig, Ritterstrasse 26, 04109 Leipzig, Germany.
[b] **Author to whom correspondence should be addressed:** gregor.loisch@desy.de

ABSTRACT

Various applications in modern particle accelerators or experiments involving high energy particle beams require a gas atmosphere or involve the production of big amounts of residual gas. Among these are, e.g., gas cells for plasma acceleration, gas jet targets, or plasma lenses. As high beam quality and stable operation of RF-accelerator cavities demand for ultra-high vacuum (UHV) conditions, a separation between high pressure and UHV beamline sections is needed. Commonly, this is realized by differential pumping or thin windows, the main advantages of the latter being a simple and compact setup. Nevertheless, the interaction between the window and the beam particles reduces the beam quality via scattering. In this paper, low scattering, low permeability polymer foils that can withstand pressure differences up to 1 bar are investigated as electron beam windows. Measurements, analytical considerations, and simulations on the gas permeation, radiation, and UV resistivity as well as electron beam scattering are presented.

I. INTRODUCTION

Various experiments employing high energy particle beams also involve gas cells or gas targets. Among these are, e.g., measurements of beam/plasma-interaction properties,[1,2] gas targets,[3] and plasma-based particle acceleration such as laser wakefield acceleration (LWFA)[4] and beam-driven plasma wakefield acceleration (PWFA).[5] In particular, the latter have led to an increased demand for the integration of 1–100 mbar gas cells into high brightness accelerators.[6–9] As such accelerators are operated in ultra-high vacuum (UHV) conditions to preserve beam quality and to prevent arcing in the high gradient, conventional acceleration cavities, these gas cells pose new challenges to the beamline and vacuum designs.

The common solutions, well known from, e.g., gas-strippers for heavy ion beams,[10,11] are differential pumping systems,[10] beryllium windows,[12] and plasma windows,[13] all of them having individual drawbacks: differential pumping systems require multiple pumping stages and are, therefore, expensive in terms of money and beamline space. Beryllium windows scatter beam particles due to their high target density and, therefore, degrade the beam quality. Furthermore, handling of the poisonous and carcinogenic materials, especially in the case of window breaking, is a major safety issue. Plasma windows require high electrical input power and cooling and have a limited lifetime due to electrode erosion and cannot reach high vacuum conditions. Thus, they can only be part of a combination with a differential pumping system, therefore also sharing their drawbacks.

In this paper, we propose polymer foil UHV windows with low scattering cross sections to overcome the safety problems of beryllium windows while maintaining a simple and compact setup. Gas permeation measurements, maximum pressure tests, simulated and measured scattering angles, and some considerations and measurements on radiation resistance are presented. While our focus is on the demands of PWFA applications, especially in the case of PWFA experiments at the Photo Injector Test Facility at DESY, Zeuthen site (PITZ),[6,14,15] the windows are suitable for any setup with similar constraints.

II. PITZ ELECTRON BEAM WINDOW DEMANDS

Since the main function of the foil windows is the separation of the plasma cell atmosphere from the UHV accelerator environment, the gas current $\dot{Q}$ through the windows is the crucial parameter. The gas current is given by

$$\dot{Q} = \frac{K_p \cdot A}{d} \cdot \Delta p, \tag{1}$$

where K_p is the permeation constant, A is the effective area of the window, d is the foil thickness, and Δp is the pressure difference across the window. The gas permeation through the windows should satisfy two conditions:

- the pressure inside the plasma cell should not significantly change during operation, and
- the gas current through the windows has to be so low that the vacuum pumps on the UHV side can keep the pressure below the operation threshold. For the PITZ beamline, the leak rate should not exceed 1×10^{-6} mbar L s^{-1}, otherwise compromising on the operational stability of the booster cavity.

According to Eq. (1), there are several parameters, which could be adjusted to keep the gas current below the allowed value. The window area should be as small as possible. This is restricted by the electron beam, which has to pass through without being disturbed, e.g., by wakefields generated in the metallic window holders. In the PITZ case, a diameter of 5 – 10 mm was found to be sufficient. Δp is fixed by the plasma cell properties. In view of gas permeation and tear strength (i.e., mechanical stability), the foil should be as thick as possible. Nevertheless, the thickness is restricted by the scattering of the ~23 MeV/c electron beam (see Sec. IV). The last parameter is the material itself, quantified by the permeation constant. Although permeation rates for different polymer foils can be found in the literature,[16–18] the data seem to be inconsistent, depending both on the measurement procedure and on the particular foil specimen. Therefore, a dedicated setup for permeation rate measurements was designed and built.

III. FOIL PERMEABILITY MEASUREMENTS

The setup used to measure the permeability of the different foils is shown in Fig. 1. The foil separates a chamber filled with helium from one with high vacuum connected to a leak tester. The higher the permeability of the foil, the greater the signal of the leak tester. Helium is used for these measurements due to several major advantages compared to other gases:

- fast permeation through the foils,
- easy detection, and
- low He-content in residual gas.

In addition to the signal of the leak tester, the pressure on the high vacuum side of the foil was measured. The thin and delicate foils were glued onto the surface of stainless steel spacer flanges with central holes of diameters between 5 mm and 10 mm, using dedicated vacuum glue (Torr Seal, Agilent Technologies) as shown in Fig. 2. On the upper right side, remnants of the vacuum resin can be seen in gray. The edge of the beam aperture is visible in the creases of

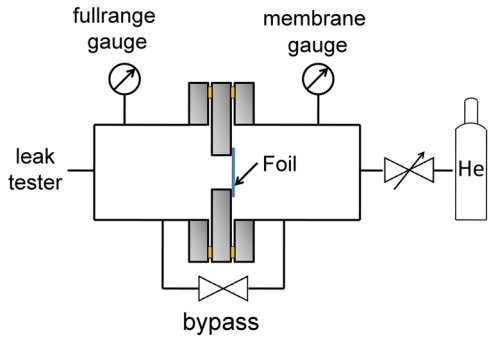

FIG. 1. Setup for measurement of gas permeation through foil windows.

the foil, which are flattened out when a one-sided pressure above ca. 5 mbar is applied. The view is from the non-metalized side of the glued foil, whereas the metallization is visible through the thin, nearly transparent PET. In the shown picture, the foil is backlighted with a bright, white lamp and the white dots in the center of the foil are caused by defects in metallization. These defects were apparent on every inspected foil, but do not seem to influence the gas permeation rate significantly.

The flange with the foil is mounted between the two chambers of the test setup using copper gaskets. The whole setup is pumped to high vacuum conditions using the membrane and turbomolecular pump of the leak tester. When a stable pressure and background signal are reached, the chambers are separated by closing the bypass valve. One side is pressurized with helium through the gas inlet to a certain pressure p_1 (typically 160 mbar), using a dosing valve.

After the pressure in the high vacuum part p_2 and the gas current $\dot{Q}$, monitored by the leak tester, are stabilized, both are measured to calculate the permeation constant K_p of the foil according to Eq. (1). Different types and thicknesses of foils with different chemical compositions and radiation lengths X_0 were tested (several samples of each).

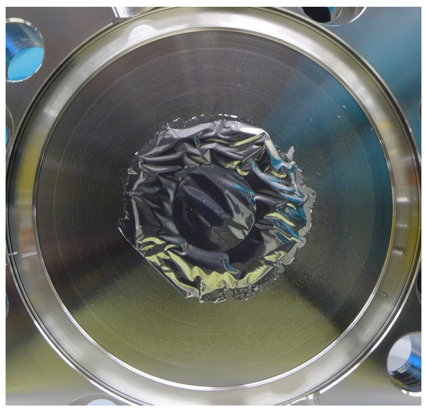

FIG. 2. Al-coated PET foil glued onto central, 10 mm diameter hole of a Conflat DN40 flange.

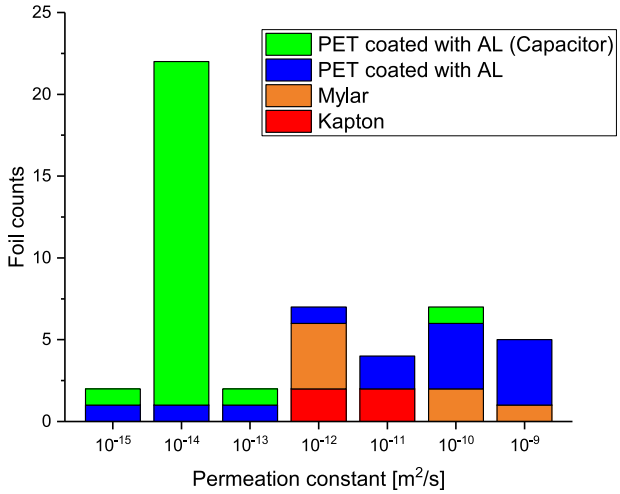

FIG. 3. Number of foils measured with different permeation constants for several kinds of tested foils.

- Kapton, 8 μm [$(C_{22}H_{10}N_2O_5)_n$, X_0 = 28.58 cm],
- Mylar, 2 μm [$(C_{10}H_8O_4)_n$, X_0 = 28.54 cm],
- PET coated with aluminum, 0.9 μm [$(C_{10}H_8O_4)_n$, X_0 = 28.54 cm], and
- PET coated with aluminum (capacitor foil), 0.9 μm, 1.9 μm, 4 μm [$(C_{10}H_8O_4)_n$, X_0 = 28.54 cm].

The aluminum coating has a thickness of 70–90 nm. It is applied to seal microscopic defects in the polymer foils, acts as a protection layer against, e.g., UV irradiation, and to improve mechanical stability.

The results of the permeation measurements are shown in Fig. 3. Whereas other foils show varying permeation constants, the capacitor foils were found to consistently provide low permeation gas windows except one sample, which was addressed to defective gluing. In addition, the permeation constant agrees for foils of all thicknesses. This suggests that the sealing is still mainly provided by the polymer foil itself, which is consistent with the small defects found in metallization, as described above.

Every foil is tested before being used in the experiment. The testing pressure of 160 mbar is chosen much higher than the operation pressure (typically several mbar). Several foils were also tested for breakdown strengths up to 1.1 bar. Whereas the Mylar foils usually break down at several 100 mbar, the thicker Kapton foils and the capacitor foil windows withstand even the full test pressure. Nevertheless, significant increase in gas permeation constants was measured for foils tested at such high pressures, which implies microscopic damage.

IV. ELECTRON BEAM SCATTERING

For PWFA experiments at PITZ, the maximum tolerable electron beam scattering introduced by the entrance electron window was simulated to be 0.2 mrad with the goal to reach the target transverse root-mean-square (rms) electron beam size of 50 μm at the beginning of the plasma channel.[19] Thin polymer foils have long radiation lengths and are mechanically sturdy, which makes them appealing as electron beam windows.

The scattering of electrons in thin films has been investigated in various theoretical,[20–22] simulation[22,23] and experimental studies.[24–26] Nevertheless, further investigation was necessary for the case in consideration here since all the above-mentioned studies investigated thin metal foils and typical scattering angles in the range of a few degrees or larger. We consider scattering of electrons under very small angles in the sub-mrad range. In this regime, the assumption of multiple scattering breaks down so that the theories developed for that realm are not valid anymore. To estimate the electron beam scattering on polymer foils, different approaches were taken:

- An analytical estimation using the multiple Coulomb scattering theory:[27]

$$\Theta_{\mathrm{RMS}} = \frac{13.6\mathrm{MeV}}{\beta c p}\sqrt{\frac{x}{X_0}}\left(1 + 0.038\ln\left(\frac{x}{X_0}\right)\right), \qquad (2)$$

  where β is the ratio of the electron velocity to the speed of light c, p is the electron momentum in MeV/c units, and x is the path length in the material.
- Scattering simulation with the FLUKA code[28,29] assuming a transverse Gaussian particle distribution and non-divergent initial electron beams with a momentum of 23 MeV/c. A single scattering model was enabled in the simulation, as the default multi-scattering model is not valid for very thin foils, where the number of elementary scatterings per simulation step is less than 20–30.[22]
- Measurements of electron scattering in the PITZ beamline. The following setup was used: the foil specimen was

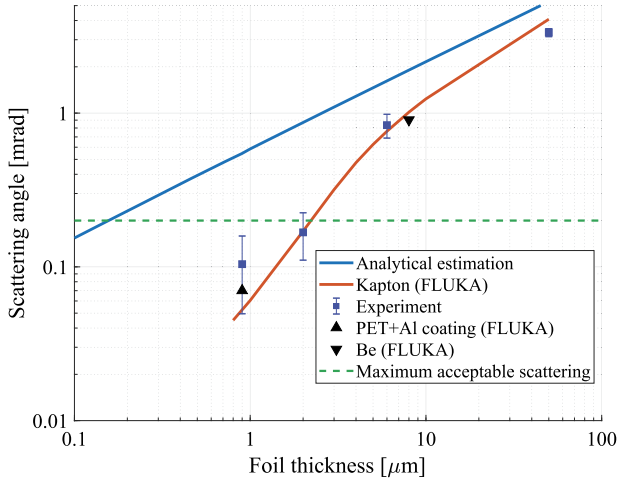

FIG. 4. Electron beam scattering at polymer foils. The analytical estimation and FLUKA simulations were performed for Kapton and an electron beam momentum of 23 MeV/c. Experiments were conducted with the following foil types: 50 μm - Kapton, 6 μm - and 1.9 μm - Mylar, and 0.9 μm - PET coated with 37.5 nm Al on both sides. The scattering value for the last foil specimen was simulated separately. The black down triangle shows the simulated scattering on a vacuum tight beryllium foil with commercially available thickness. The green dashed line shows the maximum acceptable scattering for the experiment of 0.2 mrad.

mounted on a screen station actuator; the rms beam sizes without and with foils inserted were recorded on a screen downstream of the foil to find the divergence. The scattering angle was calculated as

$$\Theta_{\mathrm{rms}} = \arctan\left(\frac{\sigma_f - \sigma_0}{L}\right), \tag{3}$$

where Θ_{rms} is the scattering angle, σ_0 is the rms size of the electron beam on the observation screen without the foil inserted, σ_f is the rms size of the electron beam with the foil inserted, and L is the distance between the foil and the observation screen.

Figure 4 shows good agreement between simulation and measurements. All methods demonstrate an exponential growth of the scattering, and simulation and experiment suggest a maximum allowable window thickness of about 1.9 μm. The analytical estimation fits well for a foil thickness of several tens of μm and more, but breaks down for thinner foils. Simulations were conducted for Kapton and PET foils. The obtained results are very similar since these materials have similar radiation lengths (see Sec. III).

V. POLYMER FOIL WINDOW RADIATION HARDNESS

In a PWFA application, several types of radiation occur, which could degrade the foil window and compromise its gas–vacuum separation capabilities. These radiation types are

- high energy electrons (can cause local heating),
- x-ray radiation from dark current of the accelerator (can lead to polymer decomposition), and
- UV-radiation from the plasma (can lead to polymer decomposition).

To quantify the influence of these on the applicability of the polymer foil windows, different calculations and experiments have been conducted.

A. Beam heating and x-ray radiation

When an electron beam passes the window foils, it deposits energy due to scattering processes. The heat is then transported from the point of beam energy deposition by radiative and conductive heat transport. Conductive heat transport was calculated to be several orders of magnitude smaller in the case of μm-thick polymer foils under consideration here. Radiative heat transport follows Planck's law,

$$P_{rad} = \sigma A T^4, \tag{4}$$

where P_{rad} is the radiated power, σ is the Stefan–Boltzmann constant, A is the radiating area, and T is the temperature of the radiator. We define the equilibrium power balance for the heated part of the foil as

$$2 * P_{rad} = P_{dep} + 2 * P_{T_0}, \tag{5}$$

where P_{dep} is the power deposited by a 1 nC, 23 MeV/c electron beam at 10 Hz repetition rate, and P_{T_0} is the power that balances the foil radiative equilibrium at room temperature T_0 = 293 K. It corresponds to the radiative power input from the surrounding surfaces. The factor of two represents the radiation of power in two directions from front- and backside of the foil (corresponding to a radiating area of 2A). P_{dep} was simulated to be 100 μW. Assuming a transverse Gaussian electron beam with an rms spot size of 0.2 mm, the maximum of the equilibrium temperature on the foil was calculated to be 51 °C. Taking into account the pulsed energy deposition by the electron bunches, the maximum transient temperature is 65 °C, which is in the range of the glass transition temperature of PET. Interpreting the one-sided metallization as a barrier for the radiated power, the maximum transient temperature could reach up to 89 °C.

Figure 5 shows a 1.9 μm thick, one-sided metalized PET foil that was exposed to an estimated 2 mC ± 0.5 mC of electron beam charge at the upstream end of a PWFA plasma cell[30] during experiments. Four spots are visible on the foil surface, which show tempering color and slight bulging. They are assumed to result from heating due to beam passage. Different spots correspond to different beam optics settings during the experiment. The surface around the spots does not show the rough structure of the surrounding foil surface. This could result from melting, glass transition or evaporation of polymer in this area. A slight increase of gas permeation was detected after the experiment using a residual gas analyzer, barely measurable in the 10^{-9} mbar pressure of the beamline vacuum. The downstream foil window shows much weaker spots, which is in agreement with the bigger spot size of the electron beam at this position.

Foil heating and radiation hardness were also tested with different types of foils in dedicated stress tests with integrated beam charges up to 7 mC. A correlation between gas permeation and beam current was found during these tests. Whereas uncoated foils were degraded in mechanical stability after exposure to electron beam and x-ray radiation of the accelerator, this did not occur with metalized foil windows. Available data was not sufficient to determine differences in radiation hardness between single-sided and two-sided metalization.

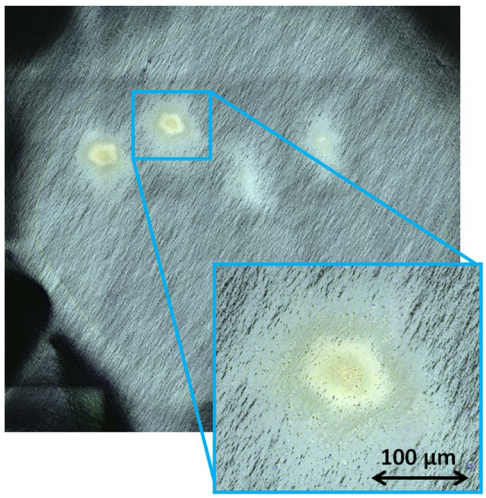

FIG. 5. Overlay of the optical and laser microscopy pictures of the polymer side of a 1.9 μm, one-sided metalized PET foil exposed to an integrated electron beam charge of 2 mC ± 0.5 mC (view from the non-metalized side). The zoom shows an alleged position of beam passage.

B. UV-radiation

The UV-hardness of the polymer foils was tested in several experiments. A 4 μm - Mylar foil window was exposed to the light of a high pressure mercury-vapor lamp with ~1 mW UV output power. An increase in gas permeation by two orders of magnitude was observed during the first 24 h of continuous irradiation. After this initial degradation, no further change in gas permeation was observed, which would still have been acceptable for the vacuum requirements of PITZ.

Metalized PET foils of several thicknesses were mounted onto a gas discharge plasma cell,[30] which was operated at 10 Hz for up to 60 h with a 60 mm distance between the window and plasma channel. No change of gas permeation was observed during these tests.

VI. CONCLUSION

In summary, we presented μm-thick polymer foils as beam windows and gas–vacuum separation in accelerator applications. Metalized PET foils of 4 μm down to <1 μm thickness were measured to provide gas permeation constants of 10^{-14} m^2/s and breakdown pressures of >1.1 bar. Beam particle scattering was simulated, measured, and proven to be acceptable for PWFA experiments.[31–33] The degradation of the foils due to exposure to typical types of radiation in accelerator applications (UV, x ray, electrons) was investigated. Negative effects, mainly caused by heating of the foil due to scattering of focused particle beams, were shown to be acceptable for the given vacuum requirements for long periods of experiments [(2 ± 0.5) mC of integrated electron beam charge, >60 h of UV and x-ray exposure], which was partially achieved by using metalized foils. Further extension of the window lifetime at lowest gas permeation should be possible by changing the position of beam passage on the foil regularly during experiments. The presented foil windows mounted onto standard vacuum flanges or vacuum valves provide a compact and cost-efficient solution for the contradictory requirements of ultra-high vacuum conditions in accelerators and particle beam experiments involving gas atmospheres of up to several 100 mbar. Widely used beryllium windows are easily outperformed in terms of safety, handling, costs, and beam scattering.

ACKNOWLEDGMENTS

The authors would like to thank Birkelbach Kondensatortechnik GmbH for the supply of high quality, metal-coated polymer foils for the presented studies.

REFERENCES

[1] J. Jacoby *et al.*, "Stopping of heavy ions in a hydrogen plasma," Phys. Rev. Lett. **74**, 1550 (1995).
[2] G. Xu *et al.*, "Determination of hydrogen density by swift heavy ions," Phys. Rev. Lett. **119**, 204801 (2017).
[3] G. G. Simon, C. Schmitt, F. Borkowski, and V. H. Walther, "Absolute electron-proton cross sections at low momentum transfer measured with a high pressure gas target system," Nucl. Phys. A **333**, 381–391 (1980).
[4] T. Tajima and J. M. Dawson, "Laser electron accelerator," Phys. Rev. Lett. **43**, 267–270 (1979).
[5] P. Chen, J. M. Dawson, R. W. Huff, and T. Katsouleas, "Acceleration of electrons by the interaction of a bunched electron beam with a plasma," Phys. Rev. Lett. **54**, 693–696 (1985).
[6] M. Gross *et al.*, "Preparations for a plasma wakefield acceleration (PWA) experiment at PITZ," Nucl. Instrum. Methods Phys. Res. A **740**, 74–80 (2014).
[7] A. Aschikhin *et al.*, "The FLASHForward facility at DESY," Nucl. Instrum. Methods Phys. Res. A **806**, 175–183 (2016).
[8] M. J. Hogan *et al.*, "Plasma wakefield acceleration experiments at FACET," New J. Phys. **12**, 055030 (2010).
[9] A. R. Rossi *et al.*, "The External-Injection experiment at the SPARC-LAB facility," Nucl. Instrum. Methods Phys. Res. A **740**, 60–66 (2014).
[10] H. Imao *et al.*, "Charge stripping of 238U ion beam by helium gas stripper," Phys. Rev. Spec. Top. - Accel. Beams **15**, 123501 (2012).
[11] G. D. Alton, R. A. Sparrow, and R. E. Olson, "Plasma as a high-charge-state projectile stripping medium," Phys. Rev. A **45**, 5957 (1992).
[12] I. Blumenfeld *et al.*, "Energy doubling of 42 GeV electrons in a metre-scale plasma wakefield accelerator," Nat. Lett. **445**, 741–744 (2007).
[13] A. Hershcovitch, "A plasma window for transmission of particle beams and radiation from vacuum to atmosphere for various applications," Phys. Plasmas **5**, 2130 (1998).
[14] F. Stephan, C. H. Boulware, M. Krasilnikov, J. Bähr *et al.*, "Detailed characterization of electron sources yielding first demonstration of european x-ray free-electron laser beam quality," Phys. Rev. Spec. Top. - Accel. Beams **13**, 020704 (2010).
[15] M. Krasilnikov, F. Stephan *et al.*, "Experimentally minimized beam emittance from an *L*-band photoinjector," Phys. Rev. Spec. Top. - Accel. Beams **15**, 100701 (2012).
[16] J. T. Hoggatt, "Investigation of the feasibility of developing low permeability polymeric films," Technical Report No. ADA304557, National Aeronautics and Space Administration, 1971.
[17] T. Makita *et al.*, "Helium gas permeability of Kapton polyimide film," Technical Report No. JAERI-M–90-137, Japan Atomic Energy Research Institute, 1990.
[18] S. J. Schowalter *et al.*, "Permeability of noble gases through Kapton, butyl, nylon, and "Silver Shield"," Nucl. Instrum. Methods Phys. Res. A **615**, 267–271 (2010).
[19] O. Lishilin *et al.*, "First results of the plasma wakefield acceleration experiment at PITZ," Nucl. Instrum. Methods Phys. Res. A **829**, 37–42 (2016).
[20] S. Goudsmit and J. L. Saunderson, "Multiple scattering of electrons," Phys. Rev. **57**, 24 (1940).
[21] C. Landron and A. Toumi, "Multiple scattering of electrons within a thin foil of aluminium," J. Phys. F: Met. Phys. **16**, 121 (1986).
[22] A. Ferrari *et al.*, "An improved multiple scattering model for charged particle transport," Nucl. Instrum. Phys. Res. B **71**, 412 (1992).
[23] M. Vilches *et al.*, "Multiple scattering of 13 and 20 MeV electrons by thin foils: A Monte Carlo study with GEANT, Geant4, and PENELOPE," Med. Phys. **36**, 3964 (2009).
[24] A. Hanson *et al.*, "Measurement of multiple scattering of 15.7 MeV electrons," Phys. Rev. **84**, 634 (1951).
[25] R. Mozley *et al.*, "Multiple scattering of 600-MeV electrons in thin foils," Phys. Rev. **111**, 647 (1958).
[26] C. Ross *et al.*, "Measurement of multiple scattering of 13 and 20 MeV electrons by thin foils," Med. Phys. **35**, 4121 (2008).
[27] H. Wiedemann, *Particle Accelerator Physics* (Springer-Verlag, Cham, Switzerland, 2015), ISBN: 978-3-319-18317-6.
[28] T. Bölen *et al.*, "The FLUKA code: Developments and challenges for high energy and medical applications," Nucl. Data Sheets **120**, 211–214 (2014).
[29] A. Ferrari *et al.*, "FLUKA: A multi-particle transport code," Technical Report No. SLAC-R-773, Stanford Linear Accelerator Center SLAC, 2005.
[30] G. Loisch *et al.*, "Jitter mitigation in low density discharge plasma cells for wakefield accelerators," J. Appl. Phys. **125**, 063301 (2019).
[31] C. A. Lindstrøm *et al.*, "Overview of the CLEAR plasma lens experiment," Nucl. Instrum. Methods Phys. Res. A **909**, 379–382 (2018).
[32] M. Gross *et al.*, "Observation of the self-modulation instability via time-resolved measurements," Phys. Rev. Lett. **120**, 144802 (2018).
[33] G. Loisch *et al.*, "Observation of high transformer ratio plasma wakefield acceleration," Phys. Rev. Lett. **121**, 064801 (2018).